

1 **Subglacial hydrological control on flow of an Antarctic Peninsula palaeo-ice stream**

2

3 Robert D. Larter^{1*}, Kelly A. Hogan¹, Claus-Dieter Hillenbrand¹, James A. Smith¹, Christine L.
4 Batchelor², Matthieu Cartigny³, Alex J. Tate¹, James D. Kirkham^{1,2}, Zoë A. Roseby^{4,1}, Gerhard Kuhn⁵,
5 Alastair G.C. Graham⁶, and Julian A. Dowdeswell²

6

7 ¹British Antarctic Survey, Madingley Road, High Cross, Cambridge CB3 0ET, UK.

8 ²Scott Polar Research Institute, University of Cambridge, Lensfield Road, Cambridge CB2 1ER, UK.

9 ³Department of Geography, South Road, Durham University, Durham DH1 3LE, UK.

10 ⁴Ocean and Earth Science, National Oceanography Centre, University of Southampton Waterfront
11 Campus, European Way, Southampton SO14 3ZH, UK.

12 ⁵Alfred Wegener Institute, Helmholtz-Centre for Polar and Marine Research, D-27568 Bremerhaven,
13 Germany.

14 ⁶College of Life and Environmental Sciences, University of Exeter, Rennes Drive, Exeter EX4 4RJ, UK

15 **Correspondence:** Robert D. Larter (rdla@bas.ac.uk).

16

17

18 **Abstract.** Basal hydrological systems play an important role in controlling the dynamic behaviour of
19 ice streams. Data showing their morphology and relationship to geological substrates beneath
20 modern ice streams are, however, sparse and difficult to collect. We present new multibeam
21 bathymetry data that make the Anvers-Hugo Trough west of the Antarctic Peninsula the most
22 completely surveyed palaeo-ice stream pathways in Antarctica. The data reveal a diverse range of
23 landforms, including streamlined features where there was fast flow in the palaeo-ice stream,
24 channels eroded by flow of subglacial water, and compelling evidence of palaeo-ice stream shear
25 margin locations. We interpret landforms as indicating that subglacial water availability played an
26 important role in facilitating ice stream flow and controlling shear margin positions. Water was likely
27 supplied to the ice stream bed episodically as a result of outbursts from a subglacial lake located in
28 the Palmer Deep basin on the inner continental shelf. These interpretations have implications for
29 controls on the onset of fast ice flow, the dynamic behaviour of palaeo-ice streams on the Antarctic
30 continental shelf, and potentially also for behaviour of modern ice streams.

31

32

33 1. Introduction

34

35 There is growing evidence that basal hydrology is a critical factor controlling the dynamic behaviour
36 of ice streams (Bell, 2008; Christianson et al., 2014; Christoffersen et al., 2014), which account for
37 most of the mass loss from large ice sheets. Understanding ice stream dynamics, including basal
38 hydrology, is thus essential for quantifying ice sheet contributions to sea level change. Subglacial
39 lakes and areas of elevated geothermal heat flux have been discovered in the onset regions of
40 several large ice streams (Fahnestock et al., 2001; Bell et al., 2007; Stearns et al., 2008). Obtaining
41 high resolution topographic data from modern ice stream beds that can reveal features associated
42 with subglacial water flow is, however, logistically difficult and time consuming (e.g. Christianson et
43 al., 2012). In contrast, modern ship-mounted sonar systems can be used to obtain such data
44 efficiently over extensive areas of former ice stream beds on continental shelves that ice has
45 retreated from since the Last Glacial Maximum (LGM; 23-19 k cal yr BP).

46 Knowledge and interpretations of submarine glacial landforms have advanced rapidly over the
47 past two decades (Dowdeswell et al., 2016). For example, it is now recognised that elongated
48 drumlins and mega-scale glacial lineations (MSGL) are signatures of past streaming ice flow on wet-
49 based, mainly sedimentary beds, and that elongation generally increases with increasingly fast past
50 flow rates (Stokes and Clark, 1999; Ó Cofaigh et al., 2002). The degree of preservation of fields of
51 MSGL and the extent to which they are overprinted by grounding zone wedges and transverse
52 moraines provides an indication to the rapidity of past grounding line retreat (Ó Cofaigh et al., 2008).
53 'Hill-hole pairs' and sediment rafts are recognised as features formed by glaciotectonic processes
54 beneath cold, dry based ice (Evans et al., 2006; Klages et al., 2015). Erosion of meandering or
55 anastomosing seabed channels and tunnel valleys with reversals of gradient along their length
56 requires a hydrological pressure gradient that indicates they could only have formed beneath
57 grounded ice (Ó Cofaigh et al., 2002; Nitsche et al., 2013). Simple hydrological pressure calculations
58 indicate that a gentle ice surface gradient produces a pressure gradient at the bed that will drive
59 water up an opposing bed slope nearly ten times as steep.

60 Modern ice sheet observations have revealed increases in ice flow rates over timescales of days
61 to years in response to Antarctic subglacial drainage events (Stearns et al., 2008; Siegfried et al.,
62 2016). Responses of glaciers in southwest Greenland to seasonal drainage of supraglacial meltwater
63 to the bed, however, show that the mode of subglacial drainage is important, as a slow-down of
64 glacier flow above a certain run-off threshold has been interpreted to correspond to a switch to
65 more efficient, channelized drainage (Sundal et al., 2011).

66 Here we present extensive new multibeam bathymetry data from the Anvers-Hugo Trough (AHT)
67 west of the Antarctic Peninsula (Fig. 1). We interpret bedforms revealed by these data as evidence of
68 a basal hydrological system that influenced the flow and lateral extent of the palaeo-ice stream and
69 was fed by a subglacial lake in a deep basin on the inner continental shelf. We use heritage
70 multichannel seismic (MCS) and deep tow boomer (DTB) data to constrain the nature of substrates
71 beneath the LGM deposits and their potential influence on the basal hydrological system and
72 sediment supply.

73

74 **1.1 Glacial history and setting**

75

76 Drilling results and seismic reflection profiles indicate that the Antarctic Peninsula Ice Sheet has
77 advanced to its western continental shelf edge many times since the late Miocene (Larter et al.,
78 1997; Barker and Camerlenghi, 2002). Through repeated glaciations the ice sheet has eroded and
79 over-deepened the inner shelf, extended the outer shelf through progradation and delivered large
80 volumes of sediment to the deep ocean (Barker and Camerlenghi, 2002; Bart and Iwai, 2012;
81 Hernández-Molina et al., 2017). The AHT, a 140 km-long by 50 km-wide cross-shelf trough (Fig. 1),
82 was a recurring ice stream pathway during glacial maxima (Larter and Cunningham, 1993; Larter and
83 Vanneste, 1995). The most recent grounding zone advance to the shelf edge along the AHT occurred
84 during the LGM (Pudsey et al., 1994; Heroy and Anderson, 2005; Ó Cofaigh et al., 2014). To the
85 southeast of the trough, the inner shelf is incised by an erosional basin, Palmer Deep (PD), that
86 measures 26 km east-to-west and 10 km north-to-south at the 800 m depth contour (Domack et al.,
87 2006; Fig. 1). PD has a maximum depth >1400 m, yet to both north and south there are small islands
88 within 12 km of its axis and there is a bank directly to its west that rises to <200 metres below sea
89 level. Rebesco et al. (1998) and Domack et al. (2006) argued that in colder temperatures than today
90 and with lower sea level – e.g. at the start of Marine Isotope Stage 2 (29 ka) - ice encroached
91 towards PD from the nearby land areas and local ice caps formed on emergent platforms around the
92 present-day islands near the basin. These authors further hypothesized that continued glacial
93 development led to the PD basin becoming completely encircled by grounded glacial ice and to
94 formation of an ice shelf over it, trapping a subglacial lake. Based on multibeam bathymetry data
95 from the inner shelf, Domack et al. (2006) described channels crossing the deepest part of the sill
96 separating the western end of PD from the AHT that are 200–500 m-wide, 100–300 m deep and
97 exhibit reversals in their longitudinal profiles. On the basis of these characteristics and similarities to
98 channels in Pine Island Bay and to the Labyrinth channels in Wright Valley in the Transantarctic
99 Mountains that had previously been interpreted as having been eroded by subglacial water flow

100 (e.g. Lowe and Anderson, 2003; Nitsche et al., 2013; Lewis et al., 2006), Domack et al. (2006)
101 interpreted the channels as having been eroded by outflow from a subglacial lake in PD. More
102 recently, geochemical analysis of pore waters from sediments in one of the basins within the
103 channel network in Pine Island Bay confirmed that it had been a sub-glacial lake (Kuhn et al., 2017).

104

105 **2. Methods**

106

107 **2.1 Multibeam bathymetry and acoustic sub-bottom profile data**

108

109 Extensive new data were collected on RRS *James Clark Ross* cruise JR284 in January 2014 using a
110 1°x1° Kongsberg EM122 system with 432 beams and a transmission frequency in the range 11.25–
111 12.75 kHz. Beam raypaths and sea bed depths were calculated in near real time using sound velocity
112 profiles derived from conductivity temperature-depth and expendable bathythermograph casts
113 made during the cruise. Processing consisted of rejecting outlying values, replacing the sound
114 velocity profile applied during acquisition with a more relevant one for some data, and gridding to
115 isometric 30 m cells using a Gaussian weighted mean filter algorithm in MB-System software (Caress
116 and Chayes, 1996; Caress et al., 2018). Pre-existing multibeam data, mostly collected on RVIB
117 *Nathaniel B. Palmer* and previous cruises of RRS *James Clark Ross* (Anderson, 2005; Domack, 2005;
118 Lavoie et al., 2015), and data along a few tracks collected more recently on HMS *Protector* using a
119 Kongsberg EM710 system (70–100 kHz), were included in the grid. Acoustic sub-bottom echo
120 sounding profiles were collected along all JR284 survey lines with a Kongsberg TOPAS PS018
121 parametric system using a 15 ms chirp transmission pulse with secondary frequencies ranging 1.3–5
122 kHz. Vessel motion and GPS navigation data on cruise JR284 were collected using a Seatex Seapath
123 200 system.

124

125 **2.2 Heritage seismic reflection data**

126

127 MCS data used were collected in the 1980s on RRS *Discovery* cruises D154 and D172 (Larter and
128 Cunningham, 1993, Larter et al., 1997). On D154, Line AMG845-03 was collected with a 2400 m-long
129 hydrophone streamer, whereas on D172 the streamer used to collect data on Line BAS878-11 was
130 800 m in length. In both cases the streamer was towed at 8–10 m depth and data were recorded
131 from 50 m-long groups with a sampling interval of 4 ms. The seismic source consisted of four airguns
132 with total volumes of 8.5 l on D154 and 15.8 l on D172, respectively, and data were processed to
133 common mid-point stack using standard procedures. Very high resolution seismic data were

134 collected using a Hunttec DTB, towed within 100 m of the sea bed, on RRS *James Clark Ross* cruise
135 JR01 in 1992 (Larter and Vanneste, 1995; Vanneste and Larter, 1995). This system transmitted a
136 broadband pulse with frequencies 0.8–10 kHz and a cycle time of 0.9 s. Data were recorded with a
137 100 μ s sampling interval from a 1 m-long hydrophone trailed behind the towed vehicle. The DTB
138 system is capable of resolving sedimentary layers <1 m in thickness and also achieves very high
139 spatial resolution due to the proximity of the source and receiver to the sea bed.

140

141 **3. Results**

142

143 **3.1 Description and interpretation of landforms and seismic/acoustic profiles.**

144

145 Integration of the new multibeam bathymetry data with pre-existing data provides nearly
146 continuous coverage of the AHT from PD to beyond the continental shelf edge, with the new data
147 spanning the full width of the trough on the middle shelf (Fig. 1). They also include coverage of the
148 confluence with a tributary trough that joins the AHT from the east on the middle shelf. We will refer
149 to this tributary by the informal name ‘Perrier Trough’, as it originates offshore from Perrier Bay,
150 Anvers Island. The data reveal extensive areas of MSGL and drumlins, which are characteristic of ice
151 stream beds and show the pattern of palaeo-ice flow (Stokes and Clark, 1999; King et al., 2009;
152 Graham et al., 2009). Fields of drumlins, with elongation ratios between 2.5 and 6:1, occur over a
153 broad transition zone between the rugged inner shelf and smoother mid-shelf part of the AHT, and
154 where the AHT crosses a structural high that separates middle and outer shelf areas (Larter et al.,
155 1997). MSGL in the mid-shelf part of the AHT have elongation ratios between 12 and 17:1, whereas
156 some on the outer shelf have elongation ratios up to 80:1. The data also confirm the occurrence of
157 several grounding zone wedges (Fig. 1), some of which had been identified previously, indicating
158 positions where the grounding zone paused during retreat from its LGM position (Larter and
159 Vanneste, 1995; Vanneste and Larter, 1995; Batchelor and Dowdeswell, 2015). Here, however, we
160 focus on two specific areas in which the landforms observed have a bearing on the role of subglacial
161 hydrology in facilitating and controlling ice stream flow.

162

163 **3.2 Southern Anvers-Hugo Trough**

164

165 In the southern part of the AHT there is a marked along-trough change in landforms across a line
166 where a MCS profile (AMG845-03) shows that a mid-shelf sedimentary basin pinches out (Figs 2a
167 and 3), with acoustic basement cropping out to the southeast (Larter et al., 1997). The acoustic

168 basement most likely represents Palaeozoic-Mesozoic igneous and metasedimentary rocks similar to
169 those that crop out on the nearby islands (Storey and Garrett, 1985; Leat et al., 1995). The
170 sedimentary strata in the basin are of unknown age, but it has previously been inferred that the
171 youngest layers could be no younger than middle Miocene and the oldest layers may be early
172 Tertiary or Late Cretaceous in age (Larter et al., 1997). Crescentic scours around the ‘upstream’ ends
173 of bathymetric highs and fields of anastomosing channels are observed in the area where acoustic
174 basement crops out (Fig. 2a). Among the anastomosing channels, the largest are up to 30 m deep
175 and 250 m wide, although many are smaller (Fig. 2b).

176 In the axis of the AHT directly north of this zone, incised into the edge of the sedimentary basin,
177 the new data reveal a set of northward shoaling and narrowing valleys spaced 2–3 km apart (Fig. 2a).
178 Individual valleys are up to 1100 m wide and 60 m deep at their southern ends (Fig. 2c), but become
179 narrower and shallower northwards (Fig. 2c,d), ultimately petering out over a distance of <5 km.
180 The slope along the steepest part of the channel axes is $\sim 2^\circ$ (Fig. 2d). In detail, the southern part of
181 each valley exhibits a v-shaped deeper section incised into a u-shaped upper section, the v-shaped
182 sections being up to 350 m wide and 45 m deep (Fig. 2c). MSGL start directly north of these valleys
183 (Figs 2a and 4) and cover most of the sea bed in the trough between this point and the continental
184 shelf edge.

185 Two acoustic sub-bottom profiles that run transverse to the trough about 8 and 10 km north of
186 the northern tips of the valleys show that the MSGL were formed in the surface of an acoustically
187 transparent layer that is draped by a 4 m-thick layer of younger sediments (Fig. 4). Where such
188 acoustically transparent layers have been cored elsewhere on the West Antarctic shelf they have
189 been shown to consist of relatively low shear strength, deformed till, dubbed ‘soft till’, and the high
190 amplitude reflector below this layer has been shown to correlate with the top of a higher shear
191 strength ‘stiff till’ (e.g. Ó Cofaigh et al., 2005a; Reinardy et al., 2011). A homogenous, terrigenous
192 diamicton with moderate shear strength, which was recovered in marine sediment cores from AHT,
193 documents the presence of the soft till there (Pudsey et al., 1994; Heroy and Anderson, 2005). Each
194 of the sub-bottom profiles shows three depressions in this high amplitude reflector that are 8–10 m
195 deep, 400–800 m wide and contain an acoustically transparent fill, above which a reflector is usually
196 observed separating the fill from the overlying soft till layer (Fig. 4).

197 We interpret the anastomosing channels and crescentic scours incised into the hard substrate on
198 the inner shelf as having been eroded by subglacial water flow at times when grounded ice extended
199 further offshore, as previous authors have interpreted similar features elsewhere (Dreimanis, 1993;
200 Lowe and Anderson, 2003; Nitsche et al., 2013; Lewis et al., 2006; Graham and Hogan, 2016). This
201 origin is also consistent with the interpretation that a subglacial lake was present in PD during the

202 last glacial period, and channels incising the sill at its western end were eroded by outflow from the
203 lake (Domack et al., 2006). Considering the scale of such features here, as well as in other areas
204 around Antarctica, and the nature of the material they are eroded into, they probably developed
205 progressively through multiple glacial cycles (Smith et al., 2009; Nitsche et al., 2013). The scale of the
206 features also implies that water flow rates fast enough to drive erosion can only have been achieved
207 through subglacial storage of water and episodic discharge (rather than continuous flow), even if it is
208 assumed that the upper parts of scours and channels were filled with ice (Nitsche et al., 2013;
209 Kirkham et al., 2019). This is, once again, consistent with the interpretation of a subglacial lake in PD,
210 and also with a semi-quantitative model that implies outbursts from trapped subglacial lakes in such
211 settings and of these approximate dimensions are likely to occur with repeat periods of the order of
212 a few centuries (Alley et al., 2006).

213 A conservative estimate for the volume of the PD subglacial lake stated by Domack et al. (2006)
214 was 20 km³. However, the full volume of the basin deeper than the sill depth of ~500 m is about 110
215 km³. If this was filled the lake would have been nearly two orders of magnitude greater in volume
216 than subglacial Lake Ellsworth (1.37 km³, Woodward et al., 2010), but still nearly two orders of
217 magnitude smaller than Lake Vostock (5400 ±1600 km³, Studinger et al., 2004). The length and width
218 of PD are similar to Lake Engelhardt, the largest of a number of connected shallow lakes beneath the
219 lower Mercer and Whillans ice streams, from which remote sensing data show ~2 km³ of water
220 drained between October 2003 and June 2006 (Fricker et al., 2007). However, water depth in these
221 lakes likely rarely exceeds 10 metres (Christianson et al., 2012), so their volumes are small compared
222 to the potential size of lakes in deep basins such as PD.

223 Considering that the northward-shoaling valleys are located in the axis of the AHT directly north
224 of an area containing anastomosing channels and crescentic scours, we interpret them as also having
225 been eroded by subglacial water flow. We interpret the upper u-shaped sections of the valleys (Fig.
226 2c) as having been widened by glacial erosion, implying that the valleys have been overridden by ice
227 since they were first carved. This is consistent with the suggestion that many features eroded into
228 bedrock on Antarctic continental shelves developed through multiple glaciations (Graham et al.,
229 2009). Even at times when there was active water flow, ice may also have filled a large part of the v-
230 shaped lower sections. Palaeo-ice flow paths indicated by streamlined bedforms show that the area
231 in the axis of the AHT where the valleys occur lies directly down flow from the sill at the western end
232 of PD. MSGL directly north of the valleys indicate that there was fast ice flow in this part of the
233 trough, likely facilitated by the soft till layer that is seen as an acoustically transparent layer in sub-
234 bottom profiles (cf. Alley et al., 1986; Ó Cofaigh et al., 2005a; Reinardy et al., 2011). The coincidence
235 of the onset of MSGL with northward disappearance of the valleys suggests that water supplied

236 through them was important in lubricating and dilating the till, thus reducing its shear strength and
237 making it more prone to deform under stress. Thus we infer that the northward terminations of the
238 valleys were associated with a transition from channelized to distributed water flow at the ice bed.
239 The shallow, filled depressions observed in the sub-bottom profiles (Fig. 4) suggest that the valleys
240 once continued further to the north, before their distal reaches were filled and the overlying soft till
241 in which MSGL are formed accumulated beneath fast-flowing ice. The sequence of units observed in
242 the profiles could have resulted from upstream migration of the onset of sediment-lubricated
243 streaming flow during the last glaciation.

244

245 **3.3 Confluence of Anvers-Hugo and Perrier troughs**

246

247 In the area of the confluence between AHT and Perrier Trough, an area of east-west aligned MSGL
248 terminates abruptly along a line parallel to their trend on the southern flank of the Perrier Trough
249 (Fig. 5a). The eastern limit of the area covered by MSGL in AHT is more irregular, but lies within a
250 band no more than 3 km wide on the eastern flank of the trough. Streamlined bedforms are absent
251 from the area between the two troughs, but several steep-sided bathymetric basins up to 1500 m
252 wide and 40 m deep are observed (Fig. 5a-c). The central parts of most basins are flat or gently-
253 dipping so that cross-sections exhibit box-shaped profiles (Fig. 5b,c). A 500 m-wide and 8 m-high
254 mound occurs on the north-western side of one of the largest basins (Fig. 5c). A few of the basins
255 span the boundary of MSGL on the southern flank of Perrier Trough. Furthermore, about 3 km north
256 of the boundary of MSGL and to the east of the other basins, linear features connect a small basin
257 ~300 m in diameter with a similarly-sized mound 1.6 km to its WNW (Fig. 5a).

258 We interpret the well-defined southern lateral boundary of MSGL in Perrier Trough as indicating
259 the marginal shear zone position when the palaeo-ice stream reached its maximum width during the
260 LGM. Similarly, the lateral limit of MSGL on the eastern flank of the AHT lies within a band that is no
261 more than 3 km wide, indicating the approximate position of the shear zone at the margin of the
262 palaeo-ice stream occupying this trough when it was at its widest. Such clear expressions of ice
263 stream shear margin positions in bed morphology have proved elusive beneath the modern ice
264 sheet, partly because the chaotic structure of shear zones causes scattering of ice-penetrating radar
265 signals that is observed as 'clutter' in survey data (Shabtaie and Bentley, 1987). The steep-sided
266 basins in the area between the two troughs are similar to the holes of hill-hole pairs and scars
267 resulting from detachment of sediment rafts observed on the northeastern part of the Amundsen
268 Sea continental shelf (Klages et al., 2013, 2015, 2016). The small mound and basin in the Perrier
269 Trough 3 km north of the boundary of MSGL appear to be a clear example of a hill-hole pair. Such

270 features are generally regarded as characteristic of erosion and deformation beneath dry-based ice
271 cover (e.g. Ottesen et al., 2005; Evans et al., 2006). The mound to the northwest of one of the largest
272 basins may represent a corresponding hill (Fig. 5a, c), although as its cross-sectional area is smaller
273 than that of the adjacent hole it cannot contain all of the excavated sediment. The absence of
274 mounds near to some of the other basins may be explained by their close proximity to the palaeo-ice
275 stream confluence, as the excavated material would only need to have been transported a short
276 distance into the path of one of the ice streams to be entrained by faster flow. Evidence of hill-hole
277 pairs having been overridden and eroded by ice after their formation has previously been reported
278 from the Norwegian continental shelf, where some hills are observed to have streamlined tails (Rise
279 et al., 2016). The pristine form of the hill-hole pair within the Perrier Trough indicates that it must
280 have formed after ice stream flow had stagnated.

281 A DTB profile runs across the bathymetric basin that lies closest to the confluence of the two
282 troughs and, beneath thin, patchily distributed younger sediments, it shows an acoustically
283 transparent layer up to 25 ms (~20 m) thick (Figs 5a, 6). This layer has a minimum thickness of <3 m
284 beneath the south-eastern edge of the basin floor, and it thickens progressively to the north-west
285 across the basin. In places short segments of truncated, dipping reflectors can be seen beneath the
286 strong reflector at the base of the acoustically transparent layer (Fig. 6). We interpret the
287 acoustically transparent layer as consisting of Quaternary diamictos overlying an unconformity
288 above mid-shelf basin sedimentary strata that are represented by the truncated, dipping reflectors.
289 The reduced thickness of the acoustically transparent layer across the basin suggests that the 'hole'
290 was formed by erosion of Quaternary diamictos and that the older sedimentary strata were
291 unaffected during its formation. As mentioned above, such holes are generally regarded as
292 characteristic of erosion beneath dry-based ice cover, and therefore the restriction of erosion to the
293 Quaternary diamictos is consistent with the shear stress threshold for brittle failure in them likely
294 being significantly lower than in the underlying consolidated strata (Evans et al., 2006). At the sea
295 bed near the foot of the steep south-east flank of the basin, a unit that is 180 m across and 7 ms
296 (~5.5 m) thick containing south-east dipping reflectors is observed. We interpret this unit as a
297 rotated slide block that has originated from the flank of the 'hole' after its excavation. The most
298 prominent reflector within the block is most likely to be from the boundary between diamicton and
299 postglacial sediment as observed to the NW of the basin (Fig. 6), in which case the displacement of
300 the block did not occur until after a layer of postglacial sediments several metres in thickness had
301 accumulated.

302 A MCS profile that runs obliquely across Perrier Trough and continues over the inter-trough area
303 shows mid-shelf basin sedimentary strata underlying the sea bed along the entire line (Figs 5a, 7). As

304 noted above, the oldest strata in this basin may be as old as Late Cretaceous, but most of the basin
305 fill is likely of Tertiary age (Larter et al., 1997). The southern lateral limit of MSGL in Perrier Trough
306 lies within 1 km of the position where a unit of younger strata with a distinct seismic facies character
307 (labelled 'later mid-shelf basin' in Fig. 7) pinches out, but is not coincident with this boundary.

308

309 **4. Discussion and Conclusions**

310

311 The features described here suggest that subglacial water, likely supplied episodically from a
312 subglacial lake in PD, played an important role in facilitating ice stream flow in the AHT during the
313 last and probably several late Quaternary glacial periods, and likely modulated the flow velocity.

314 In the palaeo-ice stream confluence area (Fig. 5a) the close juxtaposition of MSGL, which are
315 characteristic of wet-based, fast ice flow (Stokes and Clark, 1999; King et al., 2009; Graham et al.,
316 2009), with excavated basins ('holes') that are characteristic of slow, dry-based ice flow (Ottesen et
317 al., 2005; Evans et al., 2006), suggests that water availability was an important control on the lateral
318 extent of the palaeo-ice streams. This interpretation is supported by a MCS profile that shows the
319 palaeo-ice stream shear margin position on the south side of Perrier Trough does not coincide with a
320 major geological boundary (Fig. 7). The MCS profile shows that the Perrier Trough palaeo-ice stream
321 and the inter-stream area are both underlain by dipping sedimentary strata of likely Tertiary age.
322 The position of the shear margin does, however, lie within 1 km of a second-order boundary
323 between strata of different ages and with different seismic facies that may have had some influence
324 on its position (Fig. 7). Unfortunately, available seismic profiles are too widely spaced to assess how
325 closely the palaeo-shear margin follows this boundary.

326 The observation that a few of the 'holes', and one clear hill-hole pair, span the boundary of, and
327 cross-cut, MSGL on the southern flank of Perrier Trough suggests inward ice stream shear margin
328 migration during glacial recession. Lateral migration of shear margins was inferred in the area near
329 the grounding on the modern Thwaites Glacier between 1996–2000 (Rignot et al., 2002), although a
330 later study concluded that there had been no significant migration of the eastern shear margin of
331 the glacier during the most recent two decades (MacGregor et al., 2013). On different parts of the
332 northern shear margin of Whillans Ice Stream, migration rates of up to 280 ma^{-1} outwards and up to
333 170 ma^{-1} inwards were measured over the decade to 1997 (Stearns et al., 2005). Ice-penetrating
334 radar data across the northern margin of Kamb Ice Stream suggest abrupt inward migration of the
335 margin ~ 200 years before complete stagnation flow, attributed to reduced lubrication (Catania et al.,
336 2006). Reduction in basal water supply could occur due to depletion of upstream reservoirs (cf.
337 Christoffersen et al., 2014), due to surface slope reduction leading to subglacial flow

338 change/reversal, or due to ice thinning or decreasing flow rate and consequent reduction in
339 pressure melting or strain heating, respectively. Alternatively, in the case of palaeo-ice streams on
340 continental shelves, reduction in basal water supply could have resulted from total evacuation of
341 subglacial lakes trapped during ice advance at the LGM. The recovery of tills older than 13 cal. ka BP
342 at the bases of sediment cores from PD indicates that the lake there was eventually evacuated
343 (Barker & Camerlenghi 2002; Domack et al. 2001, 2006). However, water discharged from PD would
344 not have supplied the bed of the palaeo-ice stream in Perrier Trough, so lake evacuation could only
345 explain decreased water supply there if subglacial lakes were trapped in other deep basins upstream
346 of the area studied.

347 The onset of MSGL in AHT coincides with the downstream termination of the northward shoaling
348 valleys. This spatial coincidence suggests that water delivered through the channels played a role in
349 promoting streaming ice flow northward of this point. The upstream dip of 2° along the steepest
350 part of the channels (Fig. 2d) implies the minimum ice surface gradient required to produce a basal
351 hydrological pressure gradient that would drive water northward along the valleys was only 0.2° ,
352 which is within the range of surface gradients on many modern ice streams (Horgan and
353 Anandakrishnan, 2006). Water that flowed along the valleys may have been either incorporated into
354 the till layer that the MSGL formed in, thereby dilating it and facilitating shear deformation, or
355 dissipated into a thin film that spread along the ice-sediment interface (cf. Ó Cofaigh et al., 2005a).
356 The sudden appearance of MSGL at this point also requires a source for the till itself, and the most
357 obvious candidate is the underlying strata at the edge of the sedimentary basin (Fig. 3). Although
358 these strata have never been sampled they are the most likely source of reworked Cretaceous
359 radiolarians found in diamictons recovered by drilling on the outer shelf (Shipboard Scientific Party,
360 1999). Onset of MSGL where ice flowed onto a bed consisting of older sedimentary strata has also
361 been reported in other locations (e.g. Wellner et al., 2001, 2006, Graham et al., 2009). Erosion of
362 material from underlying sedimentary strata by, or in the presence of, subglacial water flow presents
363 a potential mechanism for generating a dilated basal till layer of the kind that has been shown to be
364 present beneath some modern ice streams (e.g. Alley et al., 1986; Smith, 1997).

365 Subglacial lakes in deep inshore basins such as PD are likely to form during an ice sheet growth
366 phase (Domack et al., 2006; Alley et al., 2006). In this case, episodes of water expulsion from PD may
367 have accelerated ice flow and thus contributed to rapid advance of grounded ice with a low surface
368 gradient across the shelf. Acceleration of ice flow by about 10% over 14 months was observed on
369 Byrd Glacier following a drainage event from subglacial lakes 200 km upstream of the grounding line
370 (Stearns et al., 2008), and subglacial meltwater drainage flux and routing is also known to influence
371 flow rates of glaciers in Greenland (Sundal et al., 2011). The axis of AHT shallows steadily from >600

372 m where MSGL start on the middle shelf to <440 m at the shelf edge (Vanneste and Larter, 1995),
373 and grounding lines are potentially unstable on such upstream-deepening beds (Weertman, 1974;
374 Schoof, 2007; Katz and Worster, 2010). Therefore, if episodic subglacial water outbursts caused
375 ‘surging’ ice stream behaviour, as envisaged by Alley et al. (2006), they may also have resulted in
376 fluctuations in grounding line positions.

377 Our interpretations are consistent with the hypothesis that subglacial lakes or areas of elevated
378 geothermal heat flux play a critical role in the onset of many large ice streams (Bell, 2008). There are
379 other deep, steep-sided inner shelf basins where subglacial lakes could have been trapped during
380 glacial advance in the catchment areas of several other well-documented Antarctic palaeo-ice
381 streams. For example, there are several basins >900 m deep in Marguerite Bay, which is part of the
382 catchment of the Marguerite Trough palaeo-ice stream (Livingstone et al., 2013; Arndt et al., 2013),
383 and there is a >1100 m-deep basin in Eltanin Bay at the head of the Belgica Trough palaeo-ice stream
384 (Ó Cofaigh et al., 2005b; Graham et al., 2011; Arndt et al., 2013). In the Amundsen Sea Embayment,
385 there are >1500 m-deep inner shelf basins in the catchments of both the Pine Island-Thwaites and
386 Dotson-Getz palaeo-ice streams (Larter et al., 2009; Graham et al., 2009, 2016; Nitsche et al., 2013;
387 Arndt et al., 2013; Witus et al., 2014), and it has been shown that at least one of those in the former
388 area did indeed host a sub-glacial lake (Kuhn et al., 2017). Hence subglacial lakes at the onset of
389 many continental shelf palaeo-ice streams may have facilitated their advance across the shelf during
390 late Quaternary glacial periods. Furthermore, if the lakes persisted when the ice streams had
391 advanced to the outer shelf, outbursts from them could have caused surge-like behaviour leading to
392 fluctuations in grounding line positions on typical inward-deepening Antarctic continental shelf
393 areas. Such behaviour of marine-based palaeo-ice streams on timescales of the order of centuries, as
394 suggested by the simple model proposed by Alley et al. (2006), could explain the observation of
395 cross-cutting MSGL in several outer continental shelf areas (e.g. Ó Cofaigh et al., 2005a, 2005b;
396 Mosola and Anderson, 2006). The preservation of MSGL from successive flow phases precludes
397 erosion or deposition of more than a few metres of sediment between them, which is easier to
398 envisage if the time separation between the flow phases is relatively small. The potential for such
399 subglacial lake outbursts to recur at decadal to centennial intervals and to cause significant ice
400 dynamic fluctuations means that there is a need to better understand the processes involved in
401 order to better forecast the future behaviour of modern ice streams and the contribution they will
402 make to sea-level change.

403

404 *Data availability.* The multibeam bathymetry grid is available online from the UK Polar Data Centre
405 (<https://doi.org/10.5285/70905d9c-6dc0-421b-b20b-1e2dff97e802>). The raw multibeam data and

406 acoustic sub-bottom profiler data collected on cruise JR284, as well as the heritage seismic data, are
407 available on request from the UK Polar Data Centre. Stacked MCS data from line AMG845-03 are
408 available from the Scientific Committee on Antarctic Research Seismic Data Library System
409 (<http://sdls.ogs.trieste.it/>).

410

411 *Author contributions.* RDL conceived the idea for the study and together with C-DH, JAS, JAD, KAH
412 and AGCG developed the research plan for cruise JR284. RDL together with KAH, C-DH and JAS wrote
413 the manuscript. RDL, KAH, AJT, CLB, C-DH, JAS and MC collected the multibeam bathymetry and
414 acoustic sub-bottom profile data on cruise JR284. JDK, ZAR, GK, AGCG and JAD participated in
415 discussions with the aforementioned authors on interpretation of the data and their implications for
416 subglacial hydrological systems. All authors commented on the manuscript and provided input to its
417 final version.

418

419 *Competing interests.* The authors declare that they have no conflict of interest.

420

421 *Acknowledgements.* We thank the captain, officers and crew on RRS *James Clark Ross* cruise JR284,
422 and Elanor Gowland and Ove Meisel who assisted with data collection. We also thank the captain,
423 hydrographers, officers and crew who sailed on HMS *Protector* during the 2015-16 and 2016-17
424 Antarctic seasons, from which additional data were incorporated. Heritage data collected on RVIB
425 *Nathaniel B. Palmer* were obtained from the Marine Geoscience Data System (www.marine-geo.org).
426 The MCS data on line BAS878-11 were processed by Alex Cunningham, and Christian dos
427 Santos Ferreira provided valuable help and advice in using MB-System to suppress some artefacts.
428 This study is part of the Polar Science for Planet Earth Programme of the British Antarctic Survey.
429 Participation of KAH, CLB and MC on cruise JR284 was funded by Natural Environment Research
430 Council Collaborative Gearing Scheme awards. We thank Huw Horgan and an anonymous reviewer
431 for helpful reviews that improved the paper.

432

433

434 **References**

- 435 Alley, R. B., Blankenship, D. D., Bentley, C. R., and Rooney, S. T.: Deformation of till beneath ice
436 stream B, West Antarctica, *Nature*, 322, 57–59, 1986.
- 437 Alley, R. B., Dupont, T. K., Parizek, B. R., Anandakrishnan, S., Lawson, D. E., Larson, G. J., and Evenson,
438 E. B.: Outburst flooding and the initiation of ice-stream surges in response to climatic cooling: A
439 hypothesis, *Geomorphology*, 75, 76–89, 2006.
- 440 Anderson, J.: Processed Multibeam Sonar Data (version 2) near the Antarctic Peninsula acquired
441 during Nathaniel B. Palmer expedition NBP0201 (2002), Interdisciplinary Earth Data Alliance
442 (IEDA), <https://doi.org/10.1594/IEDA/100309>, 2005.
- 443 Arndt, J. E., Schenke, H. W., Jakobsson, M., Nitsche, F. O., Buys, G., Goleby, B., Rebesco, M., Bohoyo,
444 F., Hong, J., Black, J., Greku, R., Udintsev, G., Barrios, F., Reynoso-Peralta, W., Taisei, M., and
445 Wigley, R.: The International Bathymetric Chart of the Southern Ocean (IBCSO) Version 1.0—A
446 new bathymetric compilation covering circum-Antarctic waters, *Geophys. Res. Lett.*, 40, 3111–
447 3117, <https://doi.org/10.1002/grl.504132013>, 2013.
- 448 Barker, P. F. and Camerlenghi, A.: Glacial history of the Antarctic Peninsula from Pacific margin
449 sediments, in: *Antarctic Glacial History and Sea-Level Change*, edited by: Barker, P. F.,
450 Camerlenghi, A., Acton, G. D., and Ramsay, A. T. S., *Proceedings of the Ocean Drilling Program,*
451 *Scientific Results*, [Online], 2002), vol. 178, 1–40, [https://www-](https://www-odp.tamu.edu/publications/178_SR/synth/synth.htm)
452 [odp.tamu.edu/publications/178_SR/synth/synth.htm](https://www-odp.tamu.edu/publications/178_SR/synth/synth.htm), 2002.
- 453 Bart, P. J. and Iwai, M.: The overdeepening hypothesis: How erosional modification of the marine-
454 scape during the early Pliocene altered glacial dynamics on the Antarctic Peninsula's Pacific
455 margin, *Palaeogeogr. Palaeoclimatol. Palaeoecol.* 335–336, 42–51,
456 <https://doi.org/10.1016/j.palaeo.2011.06.010>, 2012.
- 457 Batchelor, C. L. and Dowdeswell, J. A.: Ice-sheet grounding-zone wedges (GZWs) on high-latitude
458 continental margins, *Mar. Geol.*, 363, 65–92, <https://dx.doi.org/10.1016/j.margeo.2015.02.001>,
459 2015.
- 460 Bell, R. E.: The role of subglacial water in ice-sheet mass balance, *Nat. Geosci.*, 1, 297–304,
461 <https://doi.org/10.1038/ngeo186>, 2008.
- 462 Bell, R. E., Studinger, M., Shuman, C. A., Fahnstock, M. A., and Joughin, I.: Large subglacial lakes in
463 East Antarctica at the onset of fast-flowing ice streams. *Nature*, 445, 904–907,
464 <https://doi.org/10.1038/nature05554>, 2007.
- 465 Caress, D. W. and Chayes, D. N.: Improved processing of Hydrosweep DS multibeam data on the R/V
466 Maurice Ewing, *Mar. Geophys. Res.*, 18, 631–650, 1996.

467 Caress, D. W., Chayes, D. N., and dos Santos Ferreira, C.: MB-System: Mapping the Seafloor,
468 <https://www.mbari.org/products/research-software/mb-system>, 2018.

469 Catania, G. A., Scambos, T. A., Conway, H., and Raymond, C. H.: Sequential stagnation of Kamb Ice
470 Stream, West Antarctica, *Geophys. Res. Lett.*, 33, L14502,
471 <https://doi.org/10.1029/2006GL026430>, 2006.

472 Christianson, K., Jacobel, R. W., Horgan, H. J., Anandakrishnan, S., and Alley, R. B.: Subglacial Lake
473 Whillans – Ice-penetrating radar and GPS observations of a shallow active reservoir beneath a
474 West Antarctic ice stream, *Earth Planet. Sci. Lett.*, 331–332, 237–245,
475 <https://doi.org/10.1016/j.epsl.2012.03.013>, 2012.

476 Christianson, K., Peters, L. E., Alley, R. B., Anandakrishnan, S., Jacobel, R. W., Riverman, K. L., Muto,
477 A., and Keisling, B. A.: Dilatant till facilitates ice-stream flow in northeast Greenland, *Earth
478 Planet. Sci. Lett.*, 401, 57–69, <https://doi.org/10.1016/j.epsl.2014.05.060>, 2014.

479 Christoffersen, P., Bougamont, M., Carter, S. P., Fricker, H. A., and Tulaczyk, S.: Significant
480 groundwater contribution to Antarctic ice streams hydrologic budget, *Geophys. Res. Lett.*, 41,
481 2003–2010, <https://doi.org/10.1002/2014GL059250>, 2014.

482 Domack, E.: Processed Multibeam Sonar Data (version 2) near the Antarctic Peninsula acquired
483 during Nathaniel B. Palmer expedition NBP0107 (2001), Interdisciplinary Earth Data Alliance
484 (IEDA), <https://doi.org/10.1594/IEDA/100307>, 2005.

485 Domack, E., Leventer, A., Dunbar, R., Taylor, F., Brachfeld, S., and Sjunneskog, C.: Chronology of the
486 Palmer Deep site, Antarctic Peninsula: a Holocene palaeoenvironmental reference for the
487 circum-Antarctic. *The Holocene*, 11, 1–9, <https://doi.org/10.1191/095968301673881493>, 2001.

488 Domack, E. W., Amblàs, D., Gilbert, R., Brachfeld, S., Camerlenghi, A., Rebesco, M., Canals, M., and
489 Urgeles, R.: Subglacial morphology and glacial evolution of the Palmer deep outlet system,
490 Antarctic Peninsula, *Geomorphology*, 75, 125–142,
491 <https://doi.org/10.1016/j.geomorph.2004.06.013>, 2006.

492 Dreimanis, A.: Water-eroded crescentic scours and furrows associated with subglacial flutes at
493 Breidamerkurjökull, Iceland, *Boreas*, 22, 110–112, [https://doi.org/10.1111/j.1502-
494 3885.1993.tb00170.x](https://doi.org/10.1111/j.1502-3885.1993.tb00170.x), 1993.

495 Dowdeswell, J. A., Canals, M., Jakobsson, M., Todd, B. J., Dowdeswell, E. K., and Hogan, K. A.:
496 Introduction: an atlas of submarine glacial landforms, in: *Atlas of Submarine Glacial Landforms:
497 Modern, Quaternary and Ancient*, edited by Dowdeswell, J. A., Canals, M., Jakobsson, M., Todd,
498 B. J., Dowdeswell, E. K., and Hogan, K. A., *Memoirs, Geological Society, London*, vol. 46, 3–14,
499 <https://doi.org/10.1144/M46.171>, 2016.

500 Evans, D. J. A., Phillips, E. R., Hiemstra, J. F., and Auton, C. A.: Subglacial till: formation, sedimentary
501 characteristics and classification, *Earth-Sci. Rev.*, 78, 115–176,
502 <https://doi.org/10.1016/j.earscirev.2006.04.001>, 2006.

503 Fahnestock, M., Abdalati, W., Joughin, I., Brozena, J., and Gogineni, P.: High geothermal heat flow,
504 basal melt, and the origin of rapid ice flow in central Greenland, *Science*, 294, 2338–2342, 2001.

505 Fricker, H. A., Scambos, T., Bindschadler, R., and Padman, L.: An active subglacial water system in
506 West Antarctica mapped from space, *Science*, 315, 1544–1548, 2007.

507 Graham, A. G. C. and Hogan, K. A.: Crescentic scours on palaeo-ice stream beds, in: *Atlas of*
508 *Submarine Glacial Landforms: Modern, Quaternary and Ancient*, edited by Dowdeswell, J. A.,
509 Canals, M., Jakobsson, M., Todd, B. J., Dowdeswell, E. K., and Hogan, K. A., *Memoirs, Geological*
510 *Society, London*, vol. 46, 221–222, <https://doi.org/10.1144/M46.166>, 2016.

511 Graham, A. G. C., Larter, R. D., Gohl, K., Hillenbrand, C.-D., Smith, J. A., and Kuhn, G.: Bedform
512 signature of a West Antarctic palaeo-ice stream reveals a multi-temporal record of flow and
513 substrate control, *Quat. Sci. Rev.*, 28, 2774–2793,
514 <https://doi.org/10.1016/j.quascirev.2009.07.003>, 2009.

515 Graham, A. G. C., Nitsche, F. O., and Larter, R. D.: An improved bathymetry compilation for the
516 Bellingshausen Sea, Antarctica, to inform ice-sheet and ocean models, *The Cryosphere*, 5, 95–
517 106, <https://doi.org/10.5194/tc-5-95-2011>, 2011.

518 Graham, A. G. C., Jakobsson, M., Nitsche, F. O., Larter, R. D., Anderson, J. B., Hillenbrand, C.-D., Gohl,
519 K., Klages, J. P., Smith, J. A., and Jenkins, A.: Submarine glacial-landform distribution across the
520 West Antarctic margin, from grounding line to slope: the Pine Island–Thwaites ice-stream
521 system, in: *Atlas of Submarine Glacial Landforms: Modern, Quaternary and Ancient* edited by
522 Dowdeswell, J. A., Canals, M., Jakobsson, M., Todd, B. J., Dowdeswell, E. K., and Hogan, K. A.,
523 *Memoirs, Geological Society, London*, vol. 46, 493–500, <https://doi.org/10.1144/M46.173>, 2016.

524 Hernández-Molina, F. J., Larter, R. D., and Maldonado, A.: Neogene to Quaternary Stratigraphic
525 Evolution of the Antarctic Peninsula, Pacific Margin offshore of Adelaide Island: transitions from
526 a non-glacial, through glacially-influenced to a fully glacial state, *Global Planet. Change*, 156, 80–
527 111, <https://doi.org/10.1016/j.gloplacha.2017.07.002>, 2017.

528 Heroy, D. C. and Anderson, J. B.: Ice-sheet extent of the Antarctic Peninsula region during the Last
529 Glacial Maximum (LGM)—Insights from glacial geomorphology, *Geol. Soc. Am. Bull.*, 117, 1497–
530 1512, 2005.

531 Horgan, H. J. and Anandkrishnan, S.: Static grounding lines and dynamic ice streams: Evidence from
532 the Siple Coast, West Antarctica, *Geophys. Res. Lett.* 33, L18502,
533 <https://doi.org/10.1029/2006GL027091>, 2006.

534 Katz, R. F. and Worster, M. G.: Stability of ice-sheet grounding lines, *Proc. Royal Soc. A*, 466, 1597–
535 1620, <https://doi.org/10.1098/rspa.2009.0434>, 2010.

536 King, E. C., Hindmarsh, R. C. A., and Stokes, C. R.: Formation of mega-scale glacial lineations observed
537 beneath a West Antarctic ice stream, *Nat. Geosci.*, 2, 585–588,
538 <https://doi.org/10.1038/NGEO581>, 2009.

539 Kirkham, J. D., Hogan, K. A., Larter, R. D., Arnold, N. S., Nitsche, F. O., Gollledge, N. R., and
540 Dowdeswell, J. A.: Past water flow beneath Pine Island and Thwaites Glaciers, West Antarctica,
541 *The Cryosphere Discussions*, <https://doi.org/10.5194/tc-2019-67>, 2019.

542 Klages, J. P., Kuhn, G., Hillenbrand, C.-D., Graham, A. G. C., Smith, J. A., Larter, R. D., and Gohl, K.:
543 First geomorphological record and glacial history of an inter-ice stream ridge on the West
544 Antarctic continental shelf, *Quat. Sci. Rev.*, 61, 47–61,
545 <https://doi.org/10.1016/j.quascirev.2012.11.007>, 2013.

546 Klages, J. P., Kuhn, G., Graham, A. G. C., Hillenbrand, C.-D., Smith, J. A., Nitsche, F. O., Larter, R. D.,
547 and Gohl, K.: Palaeo-ice stream pathways and retreat style in the easternmost Amundsen Sea
548 Embayment, West Antarctica, revealed by combined multibeam bathymetric and seismic data,
549 *Geomorphology*, 245, 207–222, <https://doi.org/10.1016/j.geomorph.2015.05.020>, 2015.

550 Klages, J. P., Kuhn, G., Hillenbrand, C.-D., Graham, A. G. C., Smith, J. A., Larter, R. D., and Gohl, K.: A
551 glacial landform assemblage from an inter-ice stream setting in the eastern Amundsen Sea
552 Embayment, West Antarctica, in: *Atlas of Submarine Glacial Landforms: Modern, Quaternary
553 and Ancient* edited by Dowdeswell, J. A., Canals, M., Jakobsson, M., Todd, B. J., Dowdeswell, E.
554 K., and Hogan, K. A., *Memoirs, Geological Society, London*, vol. 46, 349–352,
555 <https://doi.org/10.1144/M46.147>, 2016.

556 Kuhn, G., Hillenbrand, C.-D., Kasten, S., Smith, J. A., Nitsche, F. O., Frederichs, T., Wiers, S., Ehrmann,
557 W., Klages, J. P., and Mogollón, J. M.: Evidence for a palaeo-subglacial lake on the Antarctic
558 continental shelf, *Nat. Commun.*, 8, 15591, <https://doi.org/10.1038/ncomms15591>, 2017.

559 Larter, R. D. and Cunningham, A. P.: The depositional pattern and distribution of glacial–interglacial
560 sequences on the Antarctic Peninsula Pacific margin, *Mar. Geol.*, 109, 203–219, 1993.

561 Larter, R. D. and Vanneste, L. E.: Relict subglacial deltas on the Antarctic Peninsula outer shelf,
562 *Geology*, 23, 33–36, 1995.

563 Larter, R. D., Rebesco, M., Vanneste, L. E., Gambôa, L. A. P., and Barker, P. F.: Cenozoic tectonic,
564 sedimentary and glacial history of the continental shelf west of Graham Land, Antarctic
565 Peninsula, in: *Geology and Seismic Stratigraphy of the Antarctic Margin*, 2, edited by Barker, P. F.
566 and Cooper, A. K., *Antarctic Research Series, American Geophysical Union, Washington, DC*, vol.
567 71, 1–27, 1997.

568 Larter, R. D., Graham, A. G. C., Gohl, K., Kuhn, G., Hillenbrand, C.-D., Smith, J. A., Deen, T. J.,
569 Livermore, R. A., and Schenke, H.-W.: Subglacial bedforms reveal complex basal regime in a zone
570 of paleo-ice stream convergence, Amundsen Sea Embayment, West Antarctica, *Geology*, 37,
571 411–414, <https://doi.org/10.1130/G25505A.1>, 2009.

572 Lavoie, C., Domack, E. W., Pettit, E. C., Scambos, T. A., Larter, R. D., Schenke, H.-W., Yoo, K. C., Gutt,
573 J., Wellner, J., Canals, M., Anderson, J. B., and Ambblas, D.: Configuration of the Northern
574 Antarctic Peninsula Ice Sheet at LGM based on a new synthesis of seabed imagery, *The*
575 *Cryosphere*, 9, 613–629, <https://doi.org/10.5194/tc-9-613-2015>, 2015.

576 Leat, P. T., Scarrow, J. H., and Millar, I. L.: On the Antarctic Peninsula batholiths, *Geol. Mag.*, 132,
577 399–412, 1995.

578 Lewis, A. R., Marchant, D. R., Kowalewski, D. E., Baldwin, S. L., and Webb, L. E.: The age and origin of
579 the Labyrinth, western Dry Valleys, Antarctica: Evidence for extensive middle Miocene subglacial
580 floods and freshwater discharge to the Southern Ocean, *Geology*, 34, 513–516,
581 <https://doi.org/10.1130/G22145.1>, 2006.

582 Livingstone, S. J., Ó Cofaigh C., Stokes, C. R., Hillenbrand, C.-D., Vieli, A., and Jamieson, S. S. R.:
583 Glacial geomorphology of Marguerite Bay Palaeo-Ice stream, western Antarctic Peninsula, *J.*
584 *Maps*, 9, 558–572, <https://doi.org/10.1080/17445647.2013.829411>, 2013.

585 Lowe, A. L. and Anderson, J. B.: Evidence for abundant subglacial meltwater beneath the paleo-ice
586 sheet in Pine Island Bay, Antarctica, *J. Glaciol.*, 49, 125–138, 2003.

587 MacGregor, J. A., Catania, G. A., Conway, H., Schroeder, D. M., Joughin, I., Young, D. A., Kempf, S. D.,
588 and Blankenship, D. D.: Weak bed control of the eastern shear margin of Thwaites Glacier, West
589 Antarctica, *J. Glaciol.*, 59, 900–912, <https://doi.org/10.3189/2013JoG13J050>, 2013.

590 Mosola, A. B., and Anderson, J. B.: Expansion and rapid retreat of the West Antarctic Ice Sheet in
591 eastern Ross Sea: possible consequence of over-extended ice streams?, *Quat. Sci. Rev.*, 25,
592 2177–2196, <https://doi.org/10.1016/j.quascirev.2005.12.013>, 2006.

593 Nitsche, F. O., Gohl, K., Larter, R. D., Hillenbrand, C.-D., Kuhn, G., Smith, J. A., Jacobs, S., Anderson, J.
594 B., and Jakobsson, M.: Paleo ice flow and subglacial meltwater dynamics in Pine Island Bay, West
595 Antarctica, *Cryosphere*, 7, 249–262, <https://doi.org/10.5194/tc-7-249-2013>, 2013.

596 Ó Cofaigh C., Pudsey, C. J., Dowdeswell, J. A., and Morris, P.: Evolution of subglacial bedforms along
597 a paleo-ice stream, Antarctic Peninsula continental shelf, *Geophys. Res. Lett.*, 29, 1199,
598 <https://doi.org/10.1029/2001GL014488>, 2002.

599 Ó Cofaigh, C., Dowdeswell, J. A., Allen, C. S., Hiemstra, J., Pudsey, C. J., Evans, J., and Evans, D. J. A.:
600 Flow dynamics and till genesis associated with a marine-based Antarctic palaeo-ice stream,
601 *Quat. Sci. Rev.*, 24, 709–740, <https://doi.org/10.1016/j.quascirev.2004.10.006>, 2005a.

602 Ó Cofaigh C., Larter, R. D., Dowdeswell, J. A., Hillenbrand, C.-D., Pudsey, C. J., Evans, J., and Morris,
603 P.: Flow of the West Antarctic Ice Sheet on the continental margin of the Bellingshausen Sea at
604 the Last Glacial Maximum, *J. Geophys. Res.*, 110, B11103,
605 <https://doi.org/10.1029/2005JB003619>, 2005b.

606 Ó Cofaigh C., Dowdeswell, J. A., Evans, J., and Larter, R. D.: Geological constraints on Antarctic
607 palaeo-ice-stream retreat, *Earth Surf. Proc. and Landforms*, 33, 513–525,
608 <https://doi.org/10.1002/esp.1669>, 2008.

609 Ó Cofaigh C., Davies, B. J., Livingstone, S. J., Smith, J. A., Johnson, J. S., Hocking, E. P., Hodgson, D. A.,
610 Anderson, J. B., Bentley, M. J., Canals, M., Domack, E., Dowdeswell, J. A., Evans, J., Glasser, N. F.,
611 Hillenbrand, C.-D., Larter, R. D., Roberts, S. J., and Simms, A. R.: Reconstruction of ice-sheet
612 changes in the Antarctic Peninsula since the Last Glacial Maximum, *Quat. Sci. Rev.*, 100, 87–110,
613 <https://doi.org/10.1016/j.quascirev.2014.06.023>, 2014.

614 Ottesen, D., Dowdeswell, J. A., and Rise, L.: Submarine landforms and the reconstruction of fast-
615 flowing ice streams within a large Quaternary ice sheet: the 2500-km long Norwegian Svalbard
616 margin (57° to 80° N), *Geol. Soc. Am. Bull.*, 117, 1033–1050, <https://doi.org/10.1130/B25577.1>,
617 2005.

618 Pudsey, C. J., Barker, P. F., and Larter, R. D.: Ice sheet retreat from the Antarctic Peninsula shelf,
619 *Continental Shelf Res.*, 14, 1647–1675, 1994.

620 Rebesco, M., Camerlenghi, A., DeSantis, L., Domack, E. W., and Kirby, M.: Seismic stratigraphy of
621 Palmer Deep: a fault-bounded late Quaternary sediment trap on the inner continental shelf,
622 *Antarctic Peninsula margin*, *Mar. Geol.*, 151, 89–110, 1998.

623 Reinardy, B. I., Larter, R. D., Hillenbrand, C.-D., Murray, T., Hiemstra, J. F., and Booth, A. D.:
624 Streaming flow of an Antarctic Peninsula palaeo-ice stream, both by basal sliding and
625 deformation of substrate, *J. Glaciol.*, 57, 596–608,
626 <https://doi.org/10.3189/002214311797409758>, 2011.

627 Rignot, E., Vaughan, D. G., Schmeltz, M., Dupont, T., and MacAyeal, D.: Acceleration of Pine Island
628 and Thwaites Glaciers, West Antarctica, *Ann. Glaciol.*, 34, 189–194, 2002.

629 Rise, L., Bellec, L. V., Ottesen, D., Bøe, R., and Thorsnes, T.: Hill-hole pairs on the Norwegian
630 continental shelf, in: *Atlas of Submarine Glacial Landforms: Modern, Quaternary and Ancient*,
631 edited by Dowdeswell, J. A., Canals, M., Jakobsson, M., Todd, B. J., Dowdeswell, E. K., and Hogan,
632 K. A., *Memoirs, Geological Society, London*, vol. 46, 203–204, <https://doi.org/10.1144/M46.42>,
633 2016.

634 Schoof, C.: Ice sheet grounding line dynamics: Steady states, stability, and hysteresis, *J. Geophys.*
635 *Res.*, 112, F03S28, <https://doi.org/10.1029/2006JF000664>, 2007.

636 Siegfried, M. R., Fricker, H. A., Carter, S. P., and Tulczyk, S.: Episodic ice velocity fluctuations triggered
637 by a subglacial flood in West Antarctica, *Geophys. Res. Lett.*, 43, 2640–2648,
638 <https://doi.org/10.1002/2016GL067758>, 2016.

639 Shabtaie, S., and Bentley, C. R.: West Antarctic ice streams draining into the Ross Ice Shelf:
640 configuration and mass balance. *J. Geophys. Res.*, 92, 1311–1336, 1987.

641 Shipboard Scientific Party: Shelf Transect (Sites 1100, 1102, and 1103), in: *Proc. ODP, Init. Repts.*,
642 178, edited by Barker, P. F., Camerlenghi, A., Acton, G. D., et al., 1–83 [Online]. Available from
643 World Wide Web:
644 <http://www-odp.tamu.edu/publications/178_IR/VOLUME/CHAPTERS/CHAP_09.PDF>.
645 [Cited 2019-04-23], 1999.

646 Smith, A. M.: Basal conditions on Rutford Ice Stream, West Antarctica, from seismic observations, *J.*
647 *Geophys. Res.*, 102, 543–552, 1997.

648 Smith, J. A., Hillenbrand, C.-D., Larter, R. D., Graham, A. G. C., and Kuhn, G.: The sediment infill of
649 subglacial meltwater channels on the West Antarctic continental shelf. *Quat. Res.*, 71, 190–200,
650 <https://doi.org/10.1016/j.yqres.2008.11.005>, 2009.

651 Stearns, L. A., Jezek, K. C., and Van der Veen, C. J.: Decadal-scale variations in ice flow along Whillans
652 Ice Stream and its tributaries, West Antarctica, *J. Glaciol.*, 51, 147–157, 2005.

653 Stearns, L. A., Smith, B. E., and Hamilton, G. S.: Increased flow speed on a large East Antarctic outlet
654 glacier caused by subglacial floods, *Nat. Geosci.*, 1, 827–831, <https://doi.org/10.1038/ngeo356>,
655 2008.

656 Stokes, C. R. and Clark, C. D.: Geomorphological criteria for identifying Pleistocene ice streams, *Ann.*
657 *Glaciol.*, 28, 67–75, 1999.

658 Storey, B. C. and Garrett, S. W.: Crustal growth of the Antarctic Peninsula by accretion, magmatism
659 and extension, *Geol. Mag.*, 122, 5–14, 1985.

660 Studinger, M., Bell, R. E., and Tikku, A. A.: Estimating the depth and shape of subglacial Lake Vostok's
661 water cavity from aerogravity data, *Geophys. Res. Lett.*, 31, L12401,
662 <https://doi.org/10.1029/2004GL019801>, 2004.

663 Sundal, A. V., Shepherd, A., Nienow, P., Hanna, E., Palmer, S., and Huybrechts, P.: Melt-induced
664 speed-up of Greenland ice sheet offset by efficient subglacial drainage, *Nature*, 469, 521–524,
665 <https://doi.org/10.1038/nature09740>, 2011.

666 Vanneste, L. E and Larter, R. D.: Deep-tow boomer survey on the Antarctic Peninsula Pacific margin:
667 An investigation of the morphology and acoustic characteristics of late Quaternary sedimentary
668 deposits on the outer continental shelf and upper slope, in: *Geology and Seismic Stratigraphy of*

669 the Antarctic Margin, edited by Cooper, A. K., Barker, P. F., and Brancolini, G., Antarctic Research
670 Series, American Geophysical Union, Washington, DC, vol. 68, 97–121, 1995.

671 Wellner, J. S., Lowe, A. L., Shipp, S. S., and Anderson, J. B.: Distribution of glacial geomorphic features
672 on the Antarctic continental shelf and correlation with substrate: implications for ice behaviour,
673 *J. Glaciol.*, 47, 397–411, 2001.

674 Wellner, J. S., Heroy, D. C., and Anderson, J. B.: The death mask of the antarctic ice sheet:
675 Comparison of glacial geomorphic features across the continental shelf, *Geomorphology*, 75,
676 157–171, <https://doi.org/10.1016/j.geomorph.2005.05.015>, 2006.

677 Weertman, J.: Stability of the junction of an ice sheet and an ice shelf, *J. Glaciol.*, 13, 3–11, 1974.

678 Witus, A. E., Braneky, C. M., Anderson, J. B., Szczuciński, W., Schroeder, D. M., Blankenship, D. D.,
679 and Jakobsson, M.: Meltwater intensive glacial retreat in polar environments and investigation
680 of associated sediments: example from Pine Island Bay, West Antarctica, *Quat. Sci. Rev.*, 85, 99–
681 118, <https://doi.org/10.1016/j.quascirev.2013.11.021>, 2014.

682 Woodward, J., Smith, A. M., Ross,
683 N., Thoma, M., Corr, H. F. J., King, E. C., King, M. A., Grosfeld, K., Tranter, M., and Siegert, M. J.:
684 Location for direct access to subglacial Lake Ellsworth: An assessment of geophysical data and
685 modelling, *Geophys. Res. Lett.*, 37, L11501, doi:10.1029/2010GL042884, 2010.

686

687 **Figures**

688

689 Fig. 1. Multibeam bathymetry data over Anvers-Hugo Trough, Perrier Trough and Palmer Deep. Grid-
690 cell size 30 m, displayed with shaded relief illumination from northeast. Regional bathymetry
691 contours from IBCSO v1.0 (Arndt et al., 2013). Red dashed lines mark interpreted past grounding
692 zone positions, with earliest ones labelled GZ1–GZ3. Most upstream grounding zone in Perrier
693 Trough is labelled GZ3P, as it did not necessarily form synchronously with GZ3. Only discontinuous
694 segments of later grounding zone positions are identified in Anvers-Hugo Trough. Black boxes show
695 locations of Figs 2a and 5a. Red box on inset shows location of main figure.

696

697 Fig. 2. **a** Detail of multibeam bathymetry over the boundary of the mid-shelf basin in the southern
698 part of Anvers-Hugo Trough. Grid-cell size 30 m, displayed with shaded relief illumination from 075°.
699 Dashed red lines mark interpreted former grounding zone positions. Purple line marks location of
700 MCS profile in Fig. 3, with small dots at intervals of 10 shots and larger dots and annotations at 100-
701 shot intervals. White lines mark locations of topographic profiles in **b-d** and solid red lines mark
702 locations of acoustic sub-bottom profiles in Fig. 4. Semi-transparent pink-filled areas crossing the
703 sub-bottom profiles mark the positions of the buried channels observed in the profiles and
704 interpolated between them. Yellow dotted line outlines approximate extent of area of anastomosing
705 channels. MSGL, mega scale glacial lineations. **b** Profile across anastomosing channels. **c** Cross
706 sections of northward shoaling valleys. **d** Profile along axis of one northward shoaling valley.
707 Locations of profiles shown in **a**.

708

709 Fig. 3. Part of MCS Line AMG845-03 and interpreted line drawing, showing sedimentary basin pinch
710 out at ~SP530. Dotted grey lines labelled B on the line drawing mark prominent bubble pulse
711 reverberations following the sea-floor reflection. Location of profile, including shot point positions,
712 shown in Fig. 2a.

713

714 Fig. 4. Acoustic sub-bottom (TOPAS) profiles from the southern part of Anvers-Hugo Trough showing
715 buried, filled channels overlain by acoustically-transparent 'soft till' layer with MSGL on its surface,
716 which is in turn overlain by a thin drape of postglacial sediments. Locations of profiles shown in Fig.
717 2a.

718

719 Fig. 5. **a** Detail of multibeam bathymetry over the confluence between Anvers-Hugo Trough and
720 Perrier Trough, which joins it from the east. Grid-cell size 30 m, displayed with shaded relief

721 illumination from northeast. Black lines marks locations of topographic profiles in **b-c**. Red line marks
722 location of DTB profile in Fig. 6. Purple line marks location of MCS profile in Fig. 7, with small dots at
723 intervals of 10 shots and larger dots and annotations at 100-shot intervals. Dark blue dashed lines
724 outline selected box-shaped bathymetric basins. AHT, Anvers-Hugo Trough; MSGL, mega scale glacial
725 lineations; GZ2, GZ3P, interpreted former grounding zone positions marked by dashed red lines.
726 Orange dotted line marks lateral limit of MSGL, interpreted as position of palaeo-ice stream shear
727 margins. **b** Cross sections of box-shaped basins running approximately SW-NE (i.e. approximately
728 transverse to the inferred palaeo-ice flow direction). **c** Cross-section of one of the larger basins in an
729 approximately NW-SE direction. Locations of profiles shown in **a**.

730

731 Fig. 6. Part of DTB Line 4 across the step-sided basin that lies closest to the trough confluence. The
732 profile shows an acoustically-transparent layer of variably thickness, interpreted as Quaternary
733 diamicton, overlying a strong reflector, interpreted as an unconformity above older sedimentary
734 strata. Short segments of truncated, dipping reflectors, marked by upward pointing small arrows,
735 can be seen beneath the strong reflector at the base of the acoustically-transparent layer. Two-way
736 travel times have been corrected for the tow depth of the boomer so that they represent
737 approximate times from the sea surface. Location of profile shown in Fig. 5a.

738

739 Fig. 7. Part of MCS Line BAS878-11 and interpreted line drawing, showing the entire area of the
740 confluence between Anvers-Hugo Trough and a tributary trough is underlain by sedimentary strata,
741 and that the lateral limit of MSGL in the tributary trough lies within 1 km of the position where a unit
742 of younger strata with a distinct seismic facies character pinches out. An f-k demultiple process was
743 used to suppress the sea-floor multiple reflection on this line. Dotted grey lines labelled B on the line
744 drawing mark prominent bubble pulse reverberations following the sea-floor reflection. Location of
745 profile shown in Fig. 5a.

746

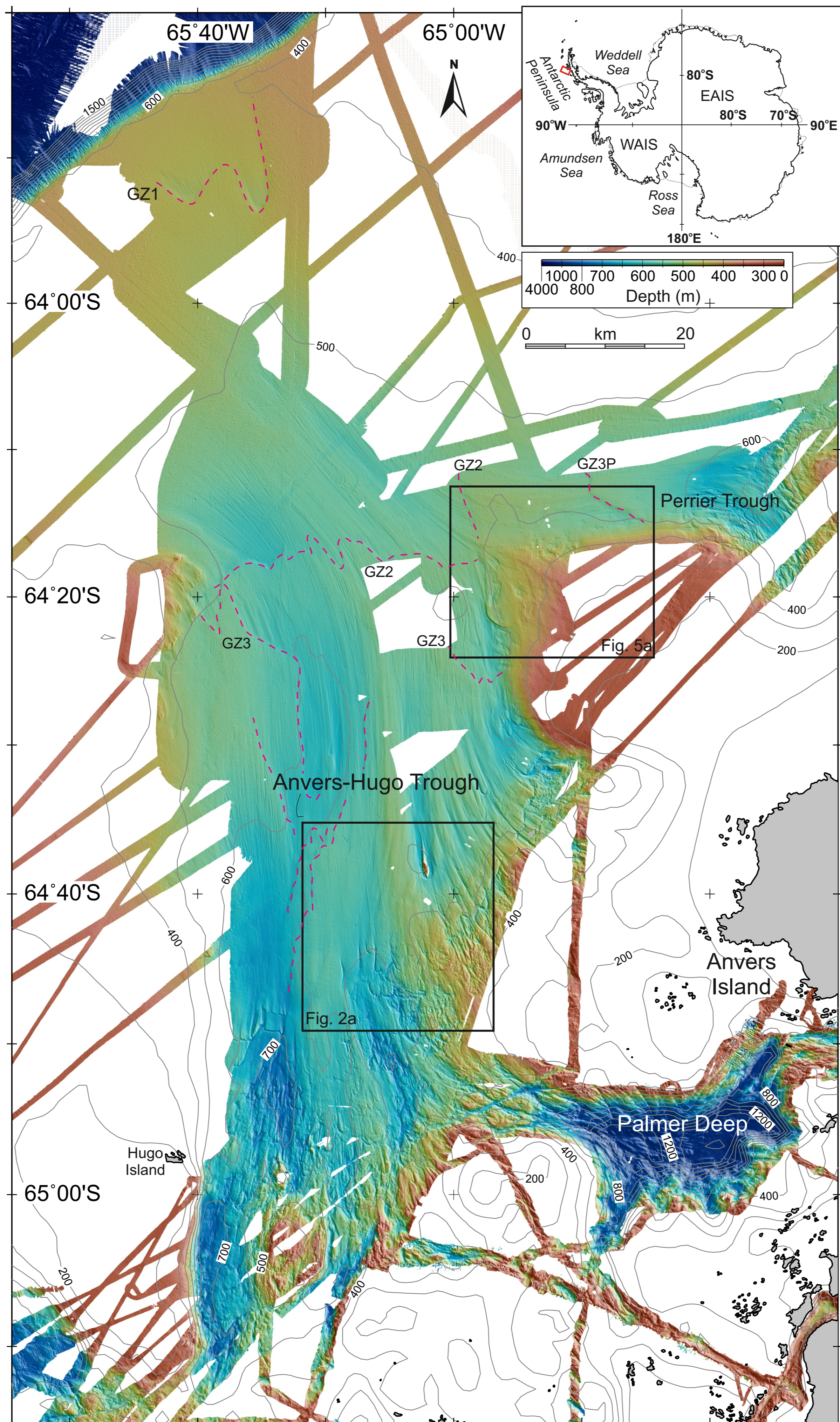


Fig. 1

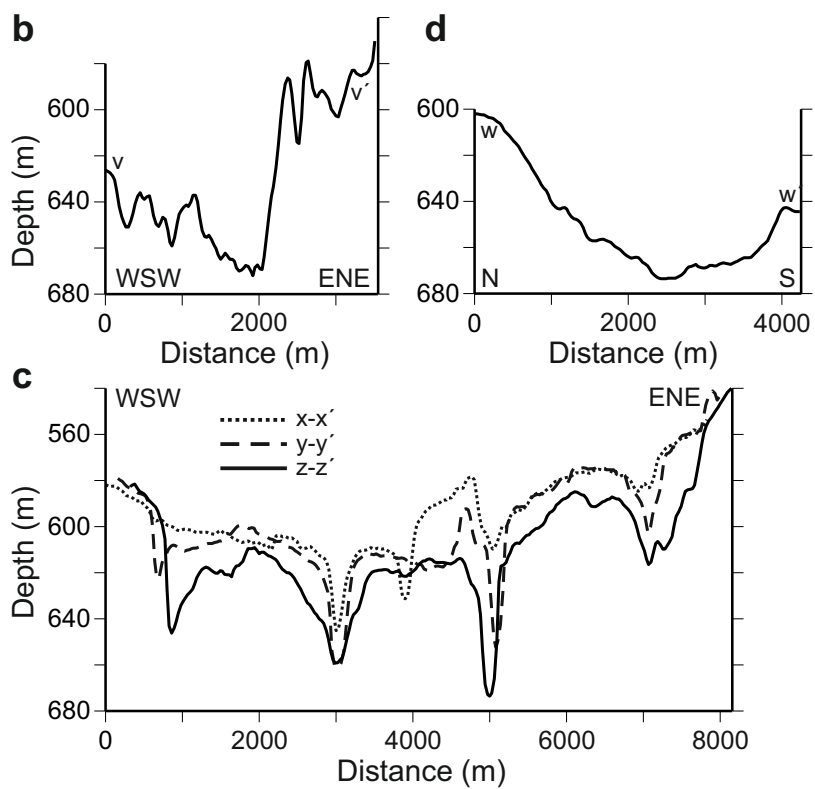
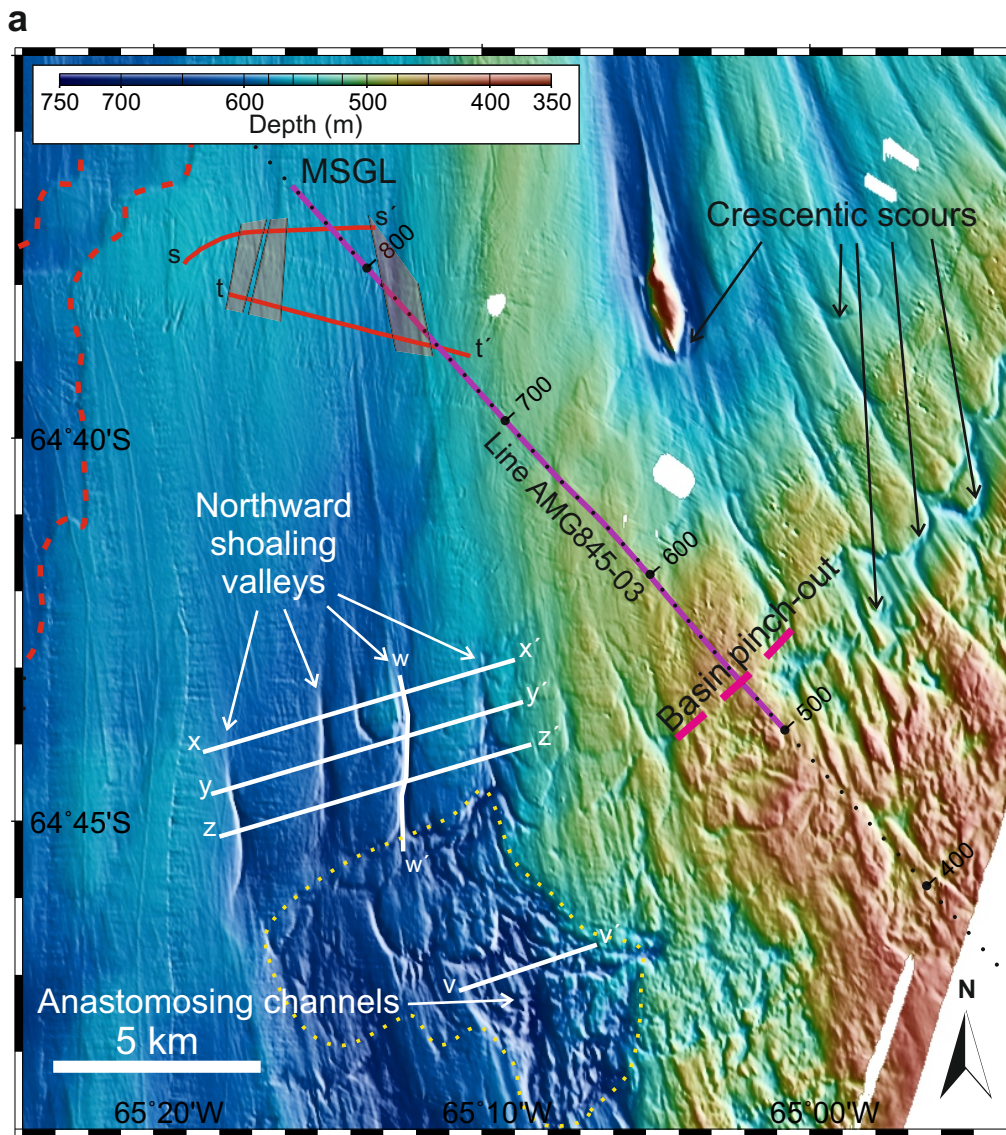


Fig. 2

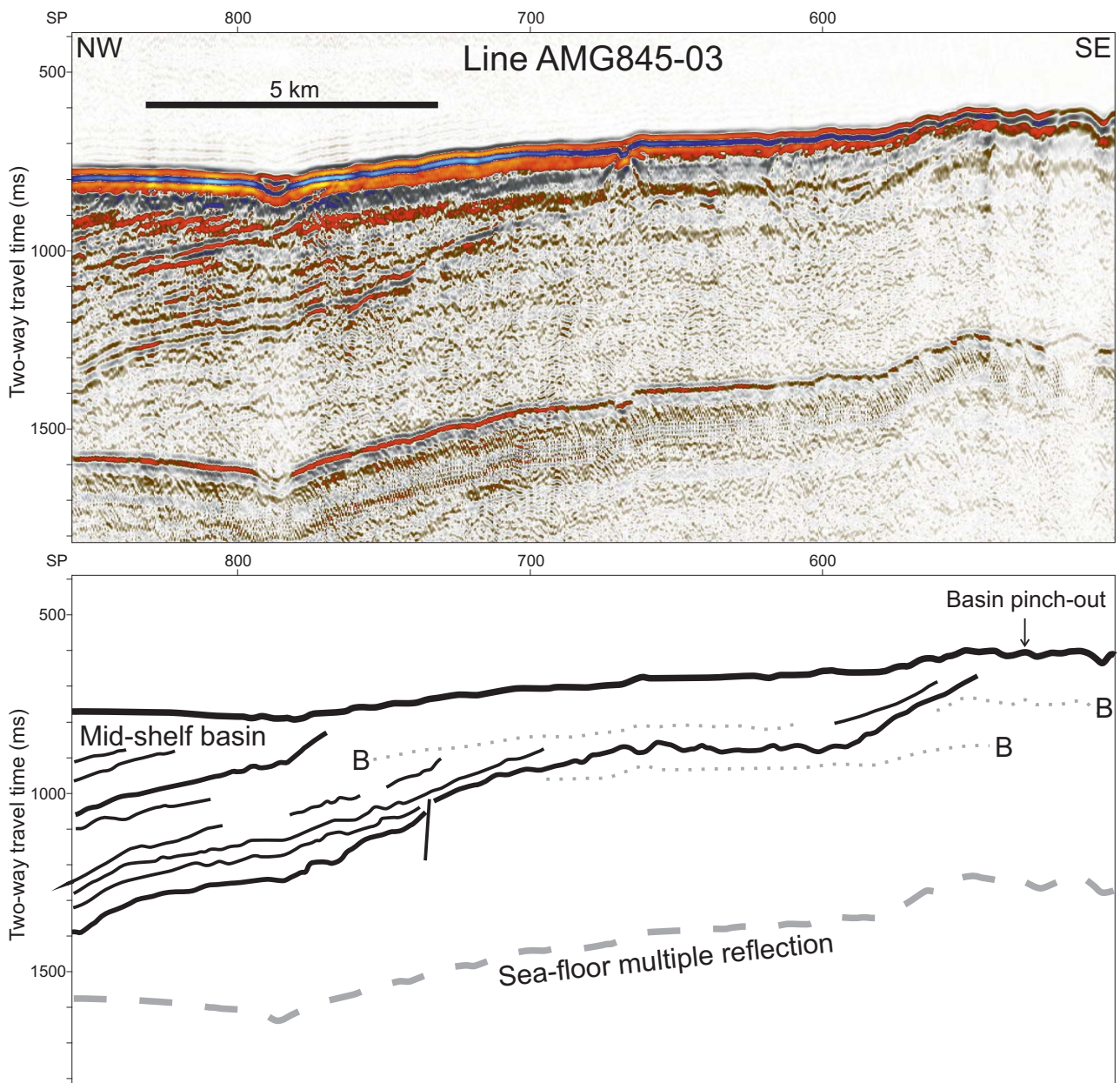


Fig. 3

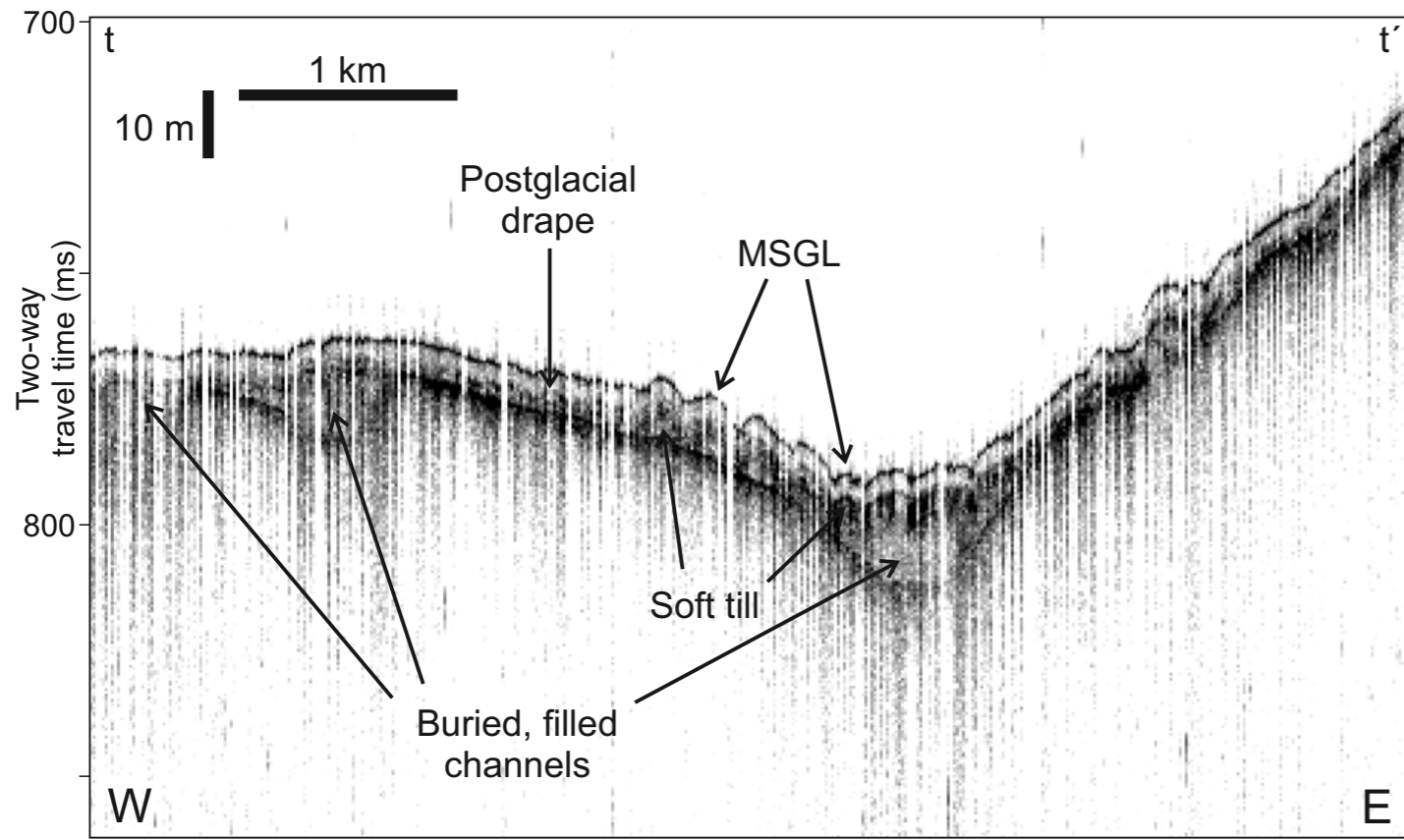
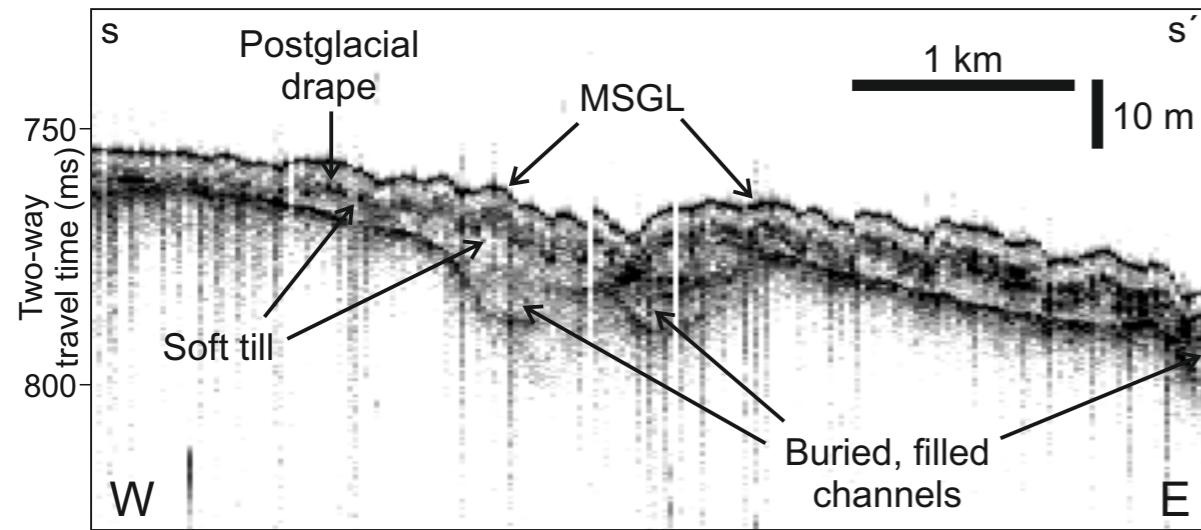


Fig. 4

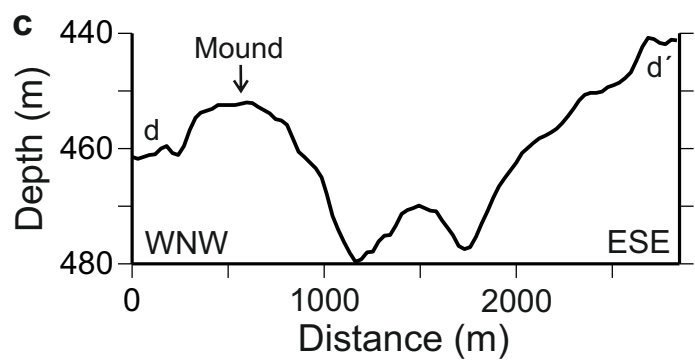
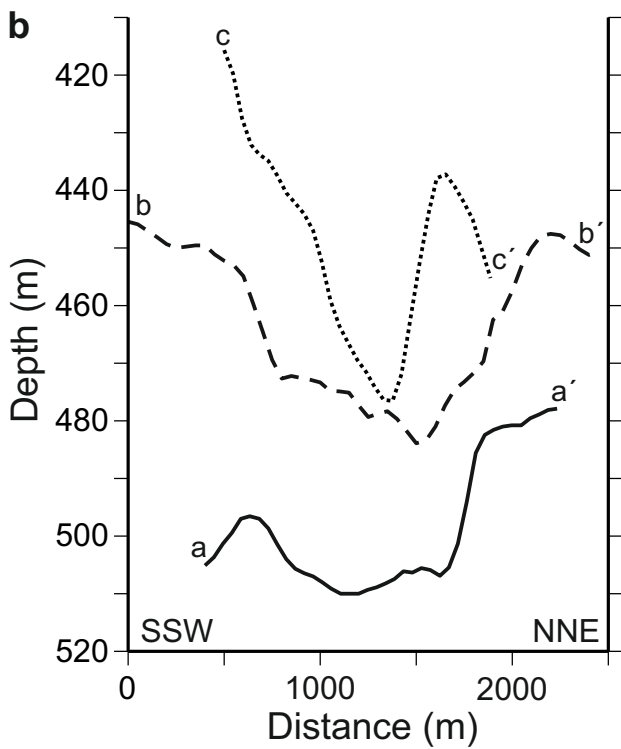
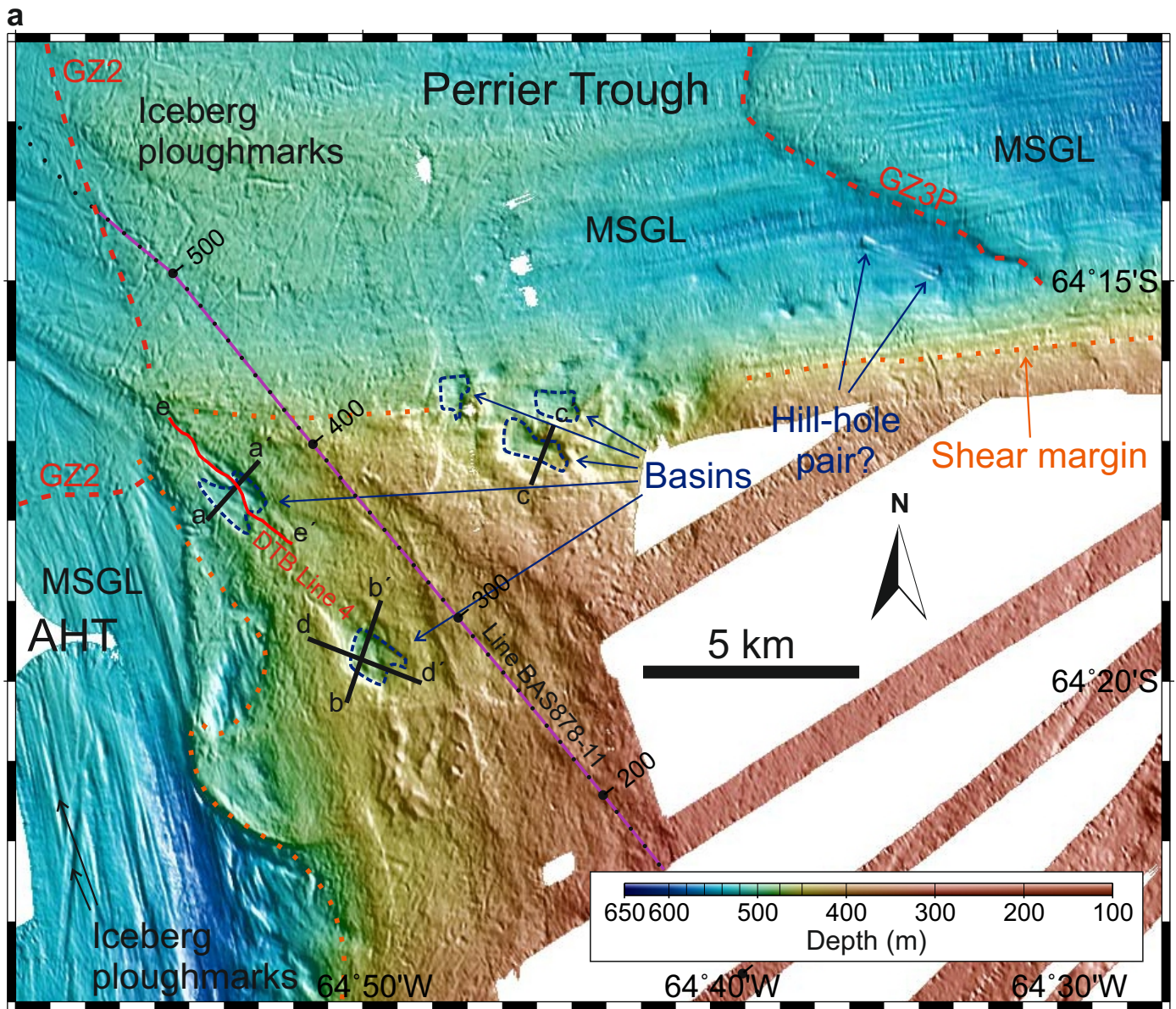


Fig. 5

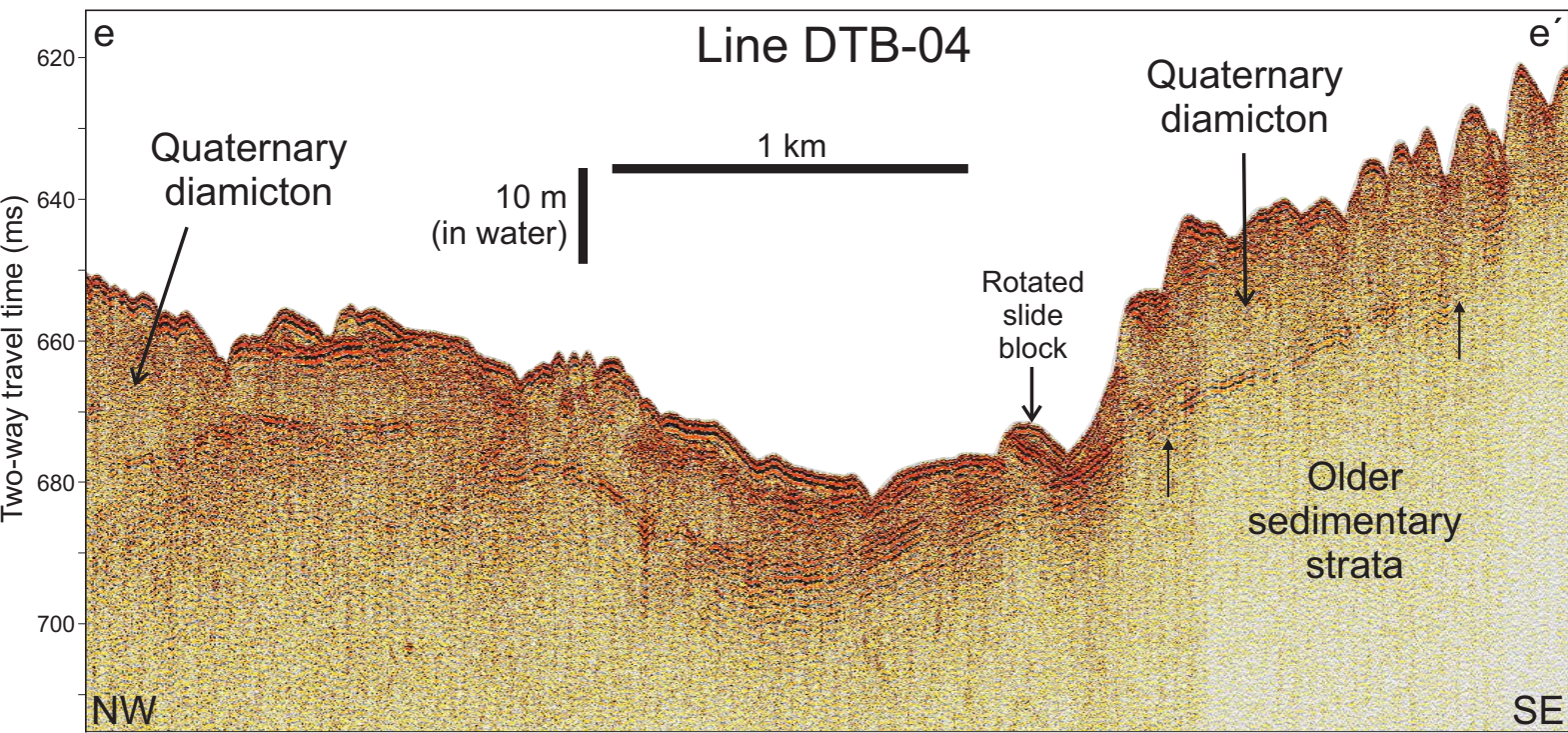


Fig. 6

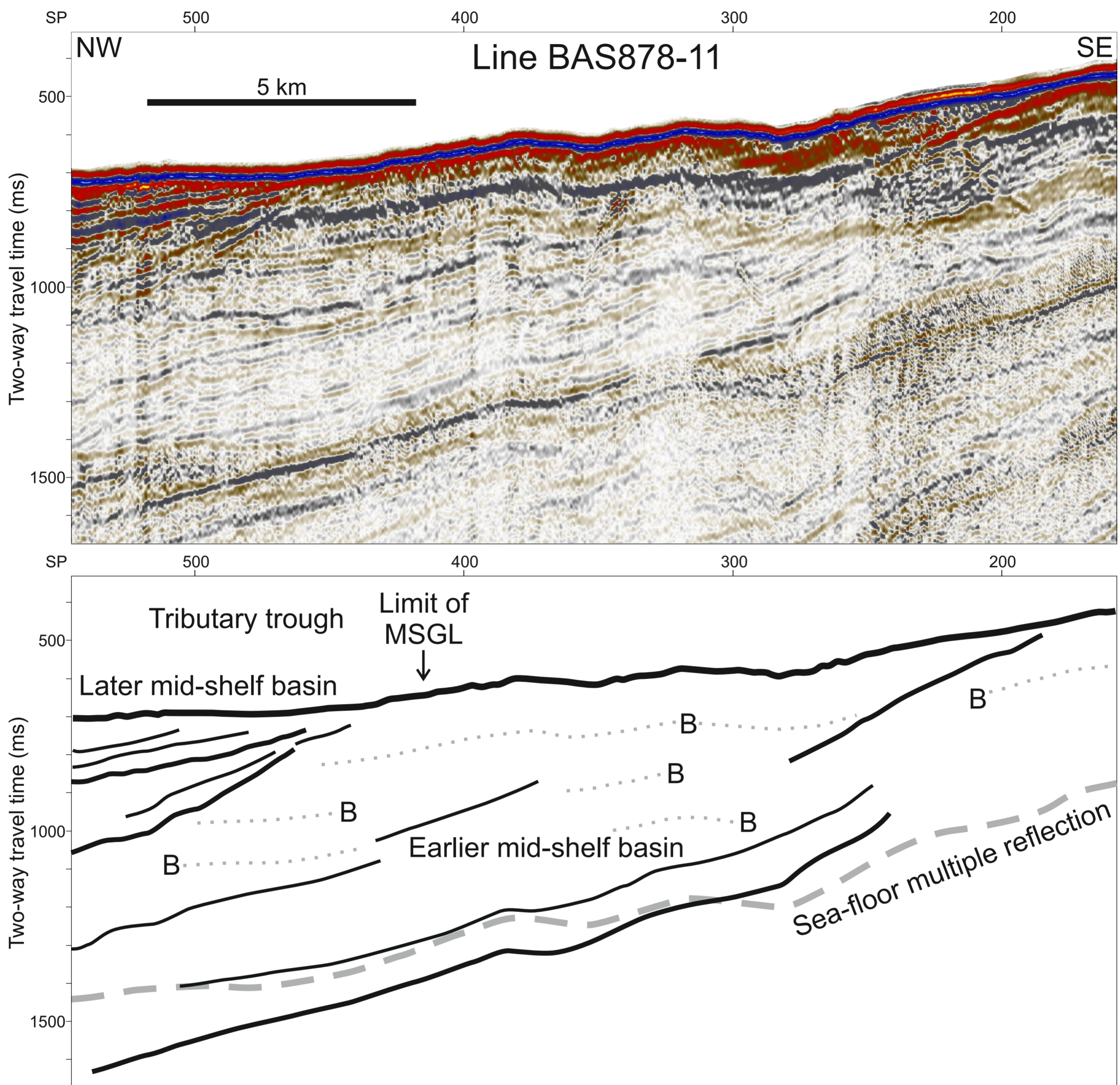


Fig. 7